Cl-Loss and H-Loss Dissociations in Low-Lying Electronic States of the CH_3Cl^+ Ion Studied Using Multiconfiguration Second-Order Perturbation Theory

Hong-Wei Xi, Ming-Bao Huang,* Bo-Zhen Chen, and Wen-Zuo Li

College of Chemistry and Chemical Engineering, Graduate School, Chinese Academy of Sciences, P.O. Box 4588, Beijing 100049, People's Republic of China

Received: January 19, 2005; In Final Form: March 10, 2005

To examine the experimentally suggested scheme of the pathways for Cl- and H-loss dissociations of the CH_3Cl^+ ion in the X^2E ($1^2A'$, $1^2A''$), A^2A_1 ($2^2A'$), and B^2E ($3^2A'$, $2^2A''$) states, the complete active space−self-consistent field (CASSCF) and multiconfiguration second-order perturbation theory (CASPT2) calculations with an atomic natural orbital (ANO) basis were performed for the $1^2A'$ (X^2A'), $1^2A''$, $2^2A'$, and $2^2A''$ states. The potential energy curves describing dissociation from the four C_s states were obtained on the basis of the CASSCF partial geometry optimization calculations at fixed C−Cl or C−H distance values, followed by the CASPT2 energy calculations. The electronic states of the CH_3^+ and CH_2Cl^+ ions produced by Cl-loss and H-loss dissociation, respectively, were carefully determined. Our calculations confirm the following experimental facts: Cl-loss dissociation occurs from the $1^2A'$ (X^2A'), $1^2A''$, and $2^2A'$ states (all leading to CH_3^+ (X^1A_1') + Cl), and H-loss dissociation does not occur from $2^2A'$. The calculations indicate that H-loss dissociation occurs from the $1^2A'$ and $1^2A''$ states (leading to CH_2Cl^+ (X^1A_1) + H and CH_2Cl^+ ($1^3A''$) + H, respectively). The calculations also indicate that H-loss dissociation occurs (with a barrier) from the $2^2A''$ state (leading to CH_2Cl^+ ($1^1A''$) + H), supporting the observation of direct dissociation from the B state to CH_2Cl^+ and that Cl-loss dissociation occurs from the $2^2A''$ state (leading to CH_3^+ ($1^3A''$) + Cl), not supporting the previously proposed Cl-loss dissociation of the B state via internal conversion of B to A. The predicted appearance potential values for CH_3^+ (X^1A_1') and CH_2Cl^+ (X^1A_1) are in good agreement with the experimental values.

I. Introduction

During the past four decades, numerous experimental studies[1−9] on the dissociation of the chloromethane ion (CH_3Cl^+) from its low-lying electronic states have been reported. These studies included measurements using photoelectron−photoion coincidence (PEPICO) spectrometry and ion photodissociation techniques. Because the electron configuration of the ground-state CH_3Cl molecule is $...(2e)^4(7a_1)^2(3e)^4$ (in C_{3v} symmetry), the X^2E [$(3e)^{-1}$], A^2A_1 [$(7a_1)^{-1}$], and B^2E [$(2e)^{-1}$] states were considered to be the three lowest-lying electronic states of the CH_3Cl^+ ion in these previous experimental studies. In 1976, Eland et al.[1] presented a general picture for the dissociation of the CH_3Cl^+ ion from the X, A, and B states (see the scheme of the fragmentation pathways drawn in ref 1), on the basis of their PEPICO experiments. They[1] observed direct dissociation from the X and A states to CH_3^+ (Cl-loss dissociation) and from the B state to CH_2Cl^+ (H-loss dissociation), but they did not observe H-loss dissociation from either the X or the A state. They[1] proposed Cl-loss dissociation of the B state via internal conversion from B to A. Several later experimental studies supported the general picture of Eland et al.[1] In 1993, Lane and Powis[6] reported their PEPICO experiments and suggested that, from the A state, Cl-loss dissociation occurs, but H-loss dissociation does not. In 2001, Won et al.[7] reported ion photodissociation experiments and suggested that the A state is a repulsive state. Olney et al.[8] (in 1996) and Locht et al.[9] (in 2001) carried out dissociative photoionization studies for CH_3Cl and measured appearance potentials (energies) for the CH_3^+ and CH_2Cl^+ ions.

In the general picture of Eland et al.,[1] the Jahn−Teller splittings of the E states (X and B) were not explicitly considered. The degeneracy of a ^2E state is removed by a Jahn−Teller distortion of the geometry from C_{3v} to C_s symmetry, giving rise to one $^2A'$ and one $^2A''$ state. Hence, the three C_{3v} states (X^2E, A^2A_1, and B^2E) of the CH_3Cl^+ ion become five C_s states: $1^2A'$, $1^2A''$, $2^2A'$, $3^2A'$, and $2^2A''$. In these experimental studies,[1−9] the excited electronic states of the CH_3^+ and CH_2Cl^+ ions as the dissociation products in the different states of CH_3Cl^+ were not considered. The appearance potentials for CH_3^+ and CH_2Cl^+ reported in refs 8 and 9 were considered to be the appearance potentials for the ground-state CH_3^+ and CH_2Cl^+ ions.

To the best of our knowledge, there is no reported theoretical study of H-loss dissociation or Cl-loss dissociation of the CH_3Cl^+ ion from different electronic states. It is known that the CASSCF (complete active space self-consistent field)[10] and CASPT2 (multiconfiguration second-order perturbation theory)[11,12] methods are useful for theoretical studies of excited electronic states of molecules and molecular ions. In the present work, we have calculated paths for H loss and Cl loss from the $1^2A'$, $1^2A''$, $2^2A'$, and $2^2A''$ states of the CH_3Cl^+ ion using the CASSCF and CASPT2 methods (the $3^2A'$ state was not studied; see below). Before we calculated the dissociation reaction paths, we calculated the geometries and energetics of the four C_s states at the CASSCF and CASPT2 levels. The geometries and energetics of the $1^2A'$ and $1^2A''$ states were previously calculated

* Corresponding author. E-mail: mbhuang1@gscas.ac.cn.

10.1021/jp050344h CCC: $30.25
Published on Web 04/27/2005

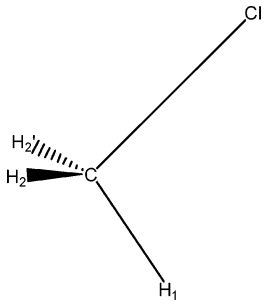

Figure 1. Atom labelings in the chloromethane ion used in the present study.

by Locht et al.[13] using the MP2 method and by Duflot et al.[14] using the CASSCF method, and we will mention the results reported in refs 13 and 14 below. In the present article, we will first briefly report our calculation results for the geometries and energetics of the four C_s states and then present a detailed description of our calculated reaction paths for H loss and Cl loss from the four C_s states. The CASSCF and CASPT2 reaction path calculations provide much information about H loss and Cl loss from the four C_s states. In the conclusion section of the present article, we relate our results to the general picture for dissociation of the CH_3Cl^+ ion in the X, A, and B states proposed by the experimental workers.

II. Calculation Details

Geometry and atom labeling used for the CH_3Cl^+ ion (C_s symmetry) are shown in Figure 1, and the H_1 atom in the symmetry plane is assumed to be the leaving species in H-loss dissociation.

The CAS (CASSCF and CASPT2) calculations were carried out using the *MOLCAS* v 5.4 quantum chemistry software.[15] With a CASSCF wavefunction constituting the reference function, the CASPT2 calculations were performed to compute the first-order wavefunction and the second-order energy in the full CI space. In the CASSCF and CASPT2 calculations, we used contracted atomic natural orbital (ANO) basis sets,[16−18] Cl (6s4p3d1f), C (5s3p2d1f), and H (3s2p1d).

The CASSCF geometry optimization calculations were performed for the $1^2A'$, $1^2A''$, $2^2A'$, and $2^2A''$ states, and the CASSCF frequency calculations were performed at the optimized geometries (using the MCLR program of *MOLCAS* v 5.4). On the basis of the CASPT2 energy calculations for the ground state ($1^2A'$) and excited states using their CASSCF optimized geometries, we obtained the CASPT2//CASSCF adiabatic excitation energies (T_0's). On the basis of the CASPT2 energy calculations for the four states at the CASSCF geometry of the ground state, we obtained the CASPT2//CASSCF vertical excitation energies (T_v's). On the basis of the CASPT2 energy calculations for the ground and excited states of the ion at the experimental geometry (R(C−Cl) = 1.776 Å, R(C−H) = 1.085 Å, ∠HCCl = 108.6°, and ∠HCClH = 120.0°)[19] of the ground-state CH_3Cl molecule, we obtained the CASPT2 relative energies (denoted as T_v''s) of the excited states to the ground state ($1^2A'$).

For Cl-loss dissociation from the $1^2A'$, $1^2A''$, $2^2A'$, and $2^2A''$ states, the C−Cl distance (R(C−Cl)) was taken as the reaction coordinate. At a set of fixed C−Cl distance values ranging from the C−Cl bond length values in the CASSCF optimized geometries of the respective states (except $2^2A'$; see section III. B) to 5.0 Å, the CASSCF partial geometry optimization calculations were performed, and then, the CASPT2 energy calculations were performed at the four sets of the partially optimized geometries. On the basis of these calculations, the CASPT2//CASSCF potential energy curves (PECs) for the Cl-loss dissociation from the $1^2A'$, $1^2A''$, $2^2A'$, and $2^2A''$ states were obtained. For H-loss dissociation, the C−H_1 distance (R(C−H_1)) was taken as the reaction coordinate. At a set of fixed C−H_1 distance values ranging from the C−H_1 bond length values in the CASSCF optimized geometries of the $1^2A'$, $1^2A''$, and $2^2A''$ states to 5.0 Å, the CASSCF partial geometry optimization calculations were performed, and then, the CASPT2 energy calculations were performed at the three sets of the partial optimized geometries. On the basis of these calculations, the CASPT2//CASSCF PECs for the H-loss dissociation from the $1^2A'$, $1^2A''$, and $2^2A''$ states were obtained. In the calculations for exploring H-loss dissociation from the $2^2A'$ state, the technical treatment was different (see section III. C).

TABLE 1: CASSCF Optimized Geometries for the $1^2A'$, $1^2A''$, $2^2A'$, and $2^2A''$ States of the CH_3Cl^+ Ion[a]

state	R(C−Cl) (Å)	R(C−H_1) (Å)	R(C−H_2) (Å)	A(H_1CCl) (°)	A(H_2CCl) (°)	D(H_2CClH_2') (°)
$1^2A'(X^2A')$	1.832	1.110	1.098	102.0	106.5	124.6
$1^2A''$	1.835	1.094	1.104.	107.2	103.8	115.8
$2^2A'$[b]						
$2^2A''$	1.926	1.096	1.182	112.4	114.5	88.2

[a] Bond length, bond angle, and dihedral angle are denoted as R, A, and D, respectively; for notations, see Figure 1. [b] A repulsive state.

We performed CASSCF calculations using the full-valence active space which includes 8 a′ (6a′−13a′) and 3 a″ (2a″−4a″) orbitals, namely, CASSCF(13,11) calculations (13 electrons and 11 active orbitals). In all the CASPT2 calculations, the weight values of the CASSCF reference functions in the first-order wavefunctions were larger than 0.8797.

The $3^2A'$ state of the CH_3Cl^+ ion was not studied in the present work because of some technical reasons. The optimized geometry and energetic results for $3^2A'$ are considered unreliable, because the frequency calculations were not successful. The PECs for Cl loss and H loss from the $3^2A'$ state were not calculated because of convergence problems in the CASSCF partial geometry optimization calculations.

III. Results and Discussion

A. Geometries and Excitation Energies. In Table 1 are given the CASSCF optimized geometries for the $1^2A'$, $1^2A''$, and $2^2A''$ states of the CH_3Cl^+ ion (for $2^2A'$, see below). There are no available experimental data for the geometries of the ground and excited states of the CH_3Cl^+ ion. In Table 2 are given the CASPT2//CASSCF T_0 and T_v values and the CASPT2 T_v' values for the four states. The CASPT2//CASSCF T_0 and T_v calculations indicate that $1^2A'$ is the ground state of the CH_3Cl^+ ion. On the basis of their accurate photoelectron spectrum, Karlsson et al.[20] reported adiabatic ionization potential (AIP) values of 11.289 and 13.8 eV and vertical ionization potential (VIP) values of 11.289 and 14.4 eV for the X^2E and A^2A_1 states of CH_3Cl^+, respectively, and reported two VIP values of 15.4 and 16.0 eV for the B^2E state. The T_0 values for the CH_3Cl^+ ion are considered to be equal to the differences between the AIP values for the excited states and the AIP value for the ground state, and therefore, the experimental T_0 value for A^2A_1 is 2.51 eV, evaluated using the experimental AIP values.[20] The T_v' values for the CH_3Cl^+ ion are considered to be equal to the differences between the VIP values for the excited states and the VIP value for the ground state, and therefore, the experimental T_v' values are 3.11 eV for A^2A_1 and 4.11 and 4.71 eV for B^2E, evaluated using the experimental VIP values.[20] All these experimental T_0 and T_v' values are listed in Table 2.

TABLE 2: CASPT2 Adiabatic (T_0) and Vertical (T_v) Excitation Energies for the $1^2A'$, $1^2A''$, $2^2A'$, and $2^2A''$ States of the CH_3Cl^+ Ion Calculated Using the CASSCF Optimized Geometries and the CASPT2 Relative Energies (T_v') Calculated at the Experimental Geometry[a] of the Ground-State CH_3Cl Molecule, Together with the Most Important Configuration (MIC) in the CASSCF Wavefunction for Each of the Four States Represented as the Ionized State of the Ground-State CH_3Cl Molecule[b]

		T_0 (eV)		T_v(eV)	T_v' (eV)	
state	MIC	calcd	exptl.[c]	calcd	calcd	exptl.[d]
$1^2A'$ (X^2A')	$[(10a')^{-1}]^e$	0.00	X^2E: 0.00	0.00	0.00	X^2E: 0.00
$1^2A''$	$[(3a'')^{-1}]^e$	0.01		0.06	−0.01	
$2^2A'$	$[(9a')^{-1}]^f$		A^2A_1: 2.51	2.85	3.18	A^2A_1: 3.11
$2^2A''$	$[(2a'')^{-1}]^e$	3.42		4.67	4.47	B^2E: 4.11, 4.71

[a] From ref 19, the experimental geometry: R(C−Cl) = 1.776 Å, R(C−H) = 1.085 Å, ∠HCCl = 108.6°, and ∠HCClH = 120.0°. [b] The electron configuration for the ground-state CH_3Cl molecule in C_s symmetry is $...(8a')^2(2a'')^2(9a')^2(10a')^2(3a'')^2$. [c] Evaluated using the experimental AIP data reported in ref 20 (the AIP value for X^2E is 11.289 eV). [d] Evaluated using the experimental VIP data reported in ref 20 (the VIP value for X^2E is 11.289 eV). [e] This state has the same MIC at the CASSCF equilibrium geometry, at the CASSCF geometry of the X^2A' state, and at the experimental geometry of the ground-state CH_3Cl molecule. [f] The repulsive $2^2A'$ state has the same MIC at the CASSCF geometry of the X^2A' state and at the experimental geometry of the ground-state CH_3Cl molecule.

The CASPT2//CASSCF T_0 calculations predict that $1^2A''$ is only 0.01 eV higher in energy than $1^2A'$, and the CASPT2//CASSCF T_v and CASPT2 T_v' values for $1^2A''$ are also very small. In the CASSCF geometries of the $1^2A'$ and $1^2A''$ states, the bond length values are quite similar, while the H_2CClH_2' dihedral angle values are significantly different. The previous MP2[13] and CASSCF[14] calculations also predicted that $1^2A''$ be slightly higher in energy than $1^2A'$. The $1^2A'$ and $1^2A''$ geometries predicted by the previous calculations[13,14] are quite different from those predicted by our CASSCF/ANO calculations. Here, we only mention the C−Cl bond lengths in the $1^2A'$ and $1^2A''$ geometries. Our CASSCF/ANO calculations predict the values of 1.832 and 1.835 Å, respectively, while the previous MP2/6-31G** calculations predicted much smaller values of 1.7671 and 1.7685 Å,[13] and the previous CASSCF calculations predicted larger values of 1.870 and 1.870 Å,[14] respectively.

The $2^2A'$ state is found to be a repulsive state about the C−Cl bond distance in the CASSCF geometry optimization calculations. Therefore, we report no CASPT2//CASSCF T_0 value for $2^2A'$ in Table 2, though the experimental AIP for A^2A_1 was reported[20] and the evaluated experimental T_0 value of 2.51 eV for $2^2A'$ is listed in Table 2. The CASPT2 T_v' value of 3.18 eV for the $2^2A'$ state is close to the experimental T_v' value of 3.11 eV for the A^2A_1 state.[20] The CASPT2//CASSCF T_0 value for $2^2A''$ is 3.42 eV (no available experimental AIP data). The CASPT2 T_v' value of 4.47 eV for $2^2A''$ is quite close to the experimental T_v' values (4.11 and 4.71 eV) for the B^2E state.[20]

The CASSCF frequency analysis calculations for $1^2A''$ and $2^2A''$ produced unique imaginary frequencies (665i and 1368i cm^{-1}, respectively) of the A″ symmetry (the previous MP2 calculations[13] also produced an imaginary frequency for $1^2A''$). The vibration modes associated with these imaginary frequencies described the rocking motions of the three hydrogen atoms, and these imaginary frequencies are not related to transition states (if any) along the Cl-loss or H-loss dissociation reaction paths for the $1^2A''$ and $2^2A''$ states (see below).

B. Cl-Loss Dissociation. In Figure 2 are given the CASPT2//CASSCF PECs for the Cl-loss dissociation from the $1^2A'$, $1^2A''$, $2^2A'$, and $2^2A''$ states of the CH_3Cl^+ ion. The CH_3Cl^+ systems of the four states at the R(C−Cl) value of 5.0 Å will be called as asymptote products of Cl-loss dissociation from the four states in the following discussion. The CASPT2//CASSCF relative energies of the asymptote products of the four states to the $1^2A'$ reactant (the $1^2A'$ state at the CASSCF equilibrium geometry) are given in parentheses. In Table 3 are listed the CASPT2//CASSCF energies of the four states at selected R(C−Cl) values, together with the charges on the Cl atom and the values of the principal geometric parameters in the CASSCF partially optimized geometries.

As shown in Table 3, the charges on the Cl atom in the asymptote products of the $1^2A'$, $1^2A''$, $2^2A'$, and $2^2A''$ states are very small (−0.001 or 0.002 e), which indicates that the products of the Cl-loss dissociation from the four states are the neutral Cl atom plus the CH_3^+ ion in different states. In Table 4 are given the CASSCF geometries and CASPT2//CASSCF relative energies (T_0's) for the $1^1A'$ ($1^1A_1'$) and $1^3A''$ states (the two lowest-lying states) of the CH_3^+ ion. The asymptote products of the $1^2A'$, $1^2A''$, and $2^2A'$ states have similar CASPT2//CASSCF energies (see Table 3 and Figure 2), and the geometries of the CH_3^+ fragment in the asymptote products of the three states (see Table 3) are almost identical to the

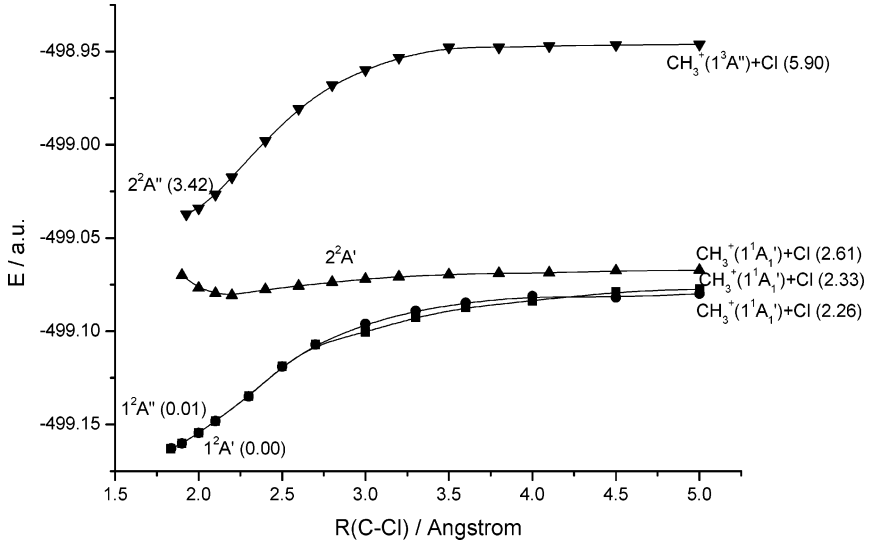

Figure 2. CASPT2//CASSCF potential energy curves for Cl-loss dissociation from the $1^2A'$, $1^2A''$, $2^2A'$, and $2^2A''$ states. In parentheses are given the CASPT2//CASSCF relative energies (in eV) of the asymptote products to the $1^2A'$ reactant.

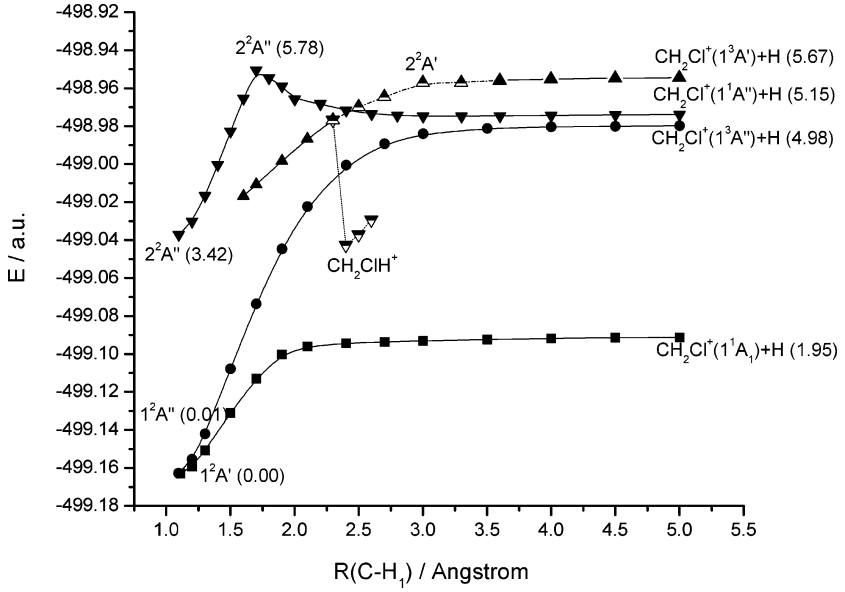

Figure 3. CASPT2//CASSCF potential energy curves for H-loss dissociation from the $1^2A'$, $1^2A''$, and $2^2A''$ states. In parentheses are given the CASPT2//CASSCF relative energies (in eV) of the asymptote products to the $1^2A'$ reactant (see calculation details and description for the $2^2A'$ curve in text).

TABLE 3: CASPT2//CASSCF Energies (*E*'s) at the Selected *R*(C−Cl) Values for the Cl-Loss Dissociation from the $1^2A'$, $1^2A''$, $2^2A'$, and $2^2A''$ States, Together with Charge Values (*Q*'s) on the Cl Atom and Values of Principal Geometric Parameters in the CASSCF Partially Optimized Geometries[a]

R(C−Cl) (Å)	*E* (a.u.)	*Q*(Cl) (e)	*R*(C−H$_2$) (Å)	*A*(H$_1$CH$_2$) (°)	*D*(H$_2$CH$_1$H$_2$′) (°)
			$1^2A'$		
1.832	−499.16301	0.659	1.098	112.1	132.8
2.0	−499.15453	0.598	1.096	115.2	141.5
2.3	−499.13488	0.436	1.095	118.2	156.4
2.7	−499.10710	0.159	1.096	119.7	171.8
3.3	−499.09254	0.038	1.097	119.9	178.7
4.0	−499.08369	0.003	1.100	120.0	179.9
5.0	−499.07735	−0.001	1.100	120.0	180.0
			$1^2A''$		
1.835	−499.16282	0.658	1.104	150.0	130.4
2.0	−499.15453	0.598	1.099	116.7	140.3
2.3	−499.13492	0.435	1.096	118.9	156.1
2.7	−499.10710	0.159	1.096	120.0	171.7
3.3	−499.08905	0.032	1.098	120.1	178.6
4.0	−499.08121	0.002	1.099	120.1	179.9
5.0	−499.07989	−0.001	1.099	120.0	179.9
			$2^2A'$		
1.9	−499.06993	0.439	1.099	117.9	151.3
2.1	−499.07962	0.346	1.097	119.0	160.4
2.4	−499.07766	0.187	1.078	119.7	172.4
2.6	−499.07565	0.144	1.080	120.0	176.4
3.0	−499.07209	0.059	1.081	120.0	179.1
3.5	−499.06966	0.018	1.081	120.0	179.7
3.8	−499.06902	0.009	1.081	120.0	179.4
4.1	−499.06868	0.004	1.081	120.0	179.4
5.0	−499.06728	0.002	1.095	120.3	179.6
			$2^2A''$		
1.926	−499.03721	0.295	1.182	116.5	90.1
2.1	−499.02668	0.240	1.183	120.1	89.8
2.4	−498.99776	0.160	1.186	123.5	85.9
2.6	−498.98059	0.115	1.187	124.7	82.5
3.0	−498.95987	0.048	1.189	125.4	77.9
3.5	−498.94955	0.005	1.196	123.8	69.2
4.1	−498.94702	−0.001	1.196	123.2	68.2
5.0	−498.94622	−0.001	1.196	123.1	68.2

[a] For notations, see Figure 1.

CASSCF geometry of the $1^1A'$ ($1^1A_1'$) ground state of the CH_3^+ ion (see Table 4). We conclude that the $1^2A'$, $1^2A''$, and $2^2A'$ states of the CH_3Cl^+ ion all correlate with the $1^1A_1'$ ground state of the CH_3^+ ion. On the basis of the CASPT2//CASSCF relative energy values given in Figure 2, the asymptote product of the $2^2A''$ state is higher in energy than the asymptote product of the $1^2A'$ state by 3.64 eV, which is very close to the CASPT2//CASSCF T_0 value of 3.56 eV for the $1^3A''$ state of the CH_3^+ ion (see Table 4). As shown in Tables 3 and 4, the geometry of the CH_3 fragment in the asymptote product of the $2^2A''$ state is very similar to the CASSCF geometry of the $1^3A''$ state of the CH_3^+ ion. We conclude that the $2^2A''$ state of the CH_3Cl^+ ion correlates with the $1^3A''$ state of the CH_3^+ ion. As shown in Figure 2, the $1^2A'$ and $1^2A''$ PECs almost coincide.

TABLE 4: CASSCF Geometries and CASPT2//CASSCF Relative Energies (T_0's) for the $1^1A'$ and $1^3A''$ States (the Two Lowest-Lying States) of the CH_3^+ Ion[a]

state	*R*(C−H$_1$) (Å)	*R*(C−H$_2$) (Å)	*A*(H$_1$CH$_2$) (°)	*D*(H$_2$CH$_1$H$_2$′) (°)	T_0 (eV)
$1^1A'$[b]	1.097	1.100	120.1[b]	179.8[b]	0.0
$1^3A''$	1.096	1.196	123.1	68.2	3.56

[a] For notations, see Figure 1. [b] The ground state of the ion is $1^1A_1'$ in D_{3h} symmetry, and our calculations within C_s symmetry did not produce the exact *A*(H$_1$CH$_2$) value of 120° and *D*(H$_2$CH$_1$H$_2$′) value of 180°.

Along the CASPT2//CASSCF PECs of the $1^2A'$, $1^2A''$, and $2^2A''$ states, the energy increases monotonically with the *R*(C−Cl) value, and there are no barriers (transition states) along the $1^2A''$ and $2^2A''$ PECs (see section III. A). The CASPT2//CASSCF energy difference between the asymptote product and the reactant for each of the three states is considered the predicted dissociation energy. The CASPT2//CASSCF dissociation energies are evaluated (using the relative energy values given in Figure 2) to be 2.33 eV for the CH_3Cl^+ ($1^2A'$) → CH_3^+ ($1^1A_1'$) + Cl dissociation, 2.25 eV for the CH_3Cl^+ ($1^2A''$) → CH_3^+ ($1^1A_1'$) + Cl dissociation, and 2.48 eV for the CH_3Cl^+ ($2^2A''$) → CH_3^+ ($1^3A''$) + Cl dissociation. We assume the appearance potential for CH_3^+ ($1^1A_1'$) (appearance potential for the production of the CH_3^+ ($1^1A_1'$) ion from CH_3Cl) to be equal to the sum of the experimental AIP value of 11.29 eV for the X^2E state[20] and the CASPT2//CASSCF dissociation energy value of 2.33 eV for the Cl-loss dissociation from the $1^2A'$ ground state, and the predicted appearance potential value of

13.62 eV for CH_3^+ ($1^1A_1'$) is quite close to the experimental values of 13.33 eV,[9] 14.0 eV,[8] and 13.43 eV (evaluated by Olney et al.[7] using experimental thermodynamic data.).

For the $2^2A'$ repulsive state, we calculated the CASPT2//CASSCF PEC starting at an R(C−Cl) value of 1.9 Å. Along the CASPT2//CASSCF PEC of the $2^2A'$ state, there seems to be a shallow minimum at an R(C−Cl) value of around 2.1 Å (see Figure 2), but we failed to find any minimum for the $2^2A'$ state in our CASSCF full geometry optimization calculations. The CASPT2//CASSCF energies of the $2^2A'$ state at the experimental geometry of the ground-state CH_3Cl molecule[19] and at the CASSCF equilibrium geometry of the ground-state CH_3Cl^+ ion are −499.045 87 and −499.058 47 au, respectively, which are both significantly higher than the CASPT2//CASSCF energies at all the selected R(C−Cl) values along the $2^2A'$ PEC (see Table 3).

C. H-Loss Dissociation. In Figure 3 are given the CASPT2//CASSCF PECs for the H-loss dissociation from the $1^2A'$, $1^2A''$, and $2^2A''$ states of the CH_3Cl^+ ion. The CH_3Cl^+ systems of the three states at the R(C−H_1) value of 5.0 Å will be called asymptote products of H-loss dissociation from the three states in the following discussion. The CASPT2//CASSCF relative energies of the asymptote products of the three states to the $1^2A'$ reactant are given in parentheses. In Table 5 are listed the CASPT2//CASSCF energies of the three states at selected R(C−H_1) values, together with the charges on the H_1 atom and the values of the principal geometric parameters in the CASSCF partially optimized geometries.

As shown in Table 5, the charges on the H_1 atom in the asymptote products of the $1^2A'$, $1^2A''$, and $2^2A''$ states are very small (0.001 e), which indicates that the products of the H-loss dissociation from the three states are the neutral H atom plus the CH_2Cl^+ ion in different states. In Table 6 are given the CASSCF geometries and CASPT2//CASSCF relative energies (T_0's) for the $1^1A'$ (1^1A_1), $1^3A''$, $1^1A''$, and $1^3A'$ states (the four lowest-lying states) of the CH_2Cl^+ ion. The $1^2A'$ ground state of the CH_3Cl^+ ion correlates with the 1^1A_1 ground state of the CH_2Cl^+ ion. As shown in Tables 5 and 6, the geometry of the CH_2Cl fragment in the asymptote product of the $1^2A'$ state is close to the CASSCF geometry of the 1^1A_1 state of the CH_2Cl^+ ion. On the basis of the CASPT2//CASSCF relative energy values given in Figure 3, the asymptote products of the $1^2A''$ and $2^2A''$ states are higher in energy than the asymptote product of the $1^2A'$ state by 3.03 and 3.20 eV, which are very close to the CASPT2//CASSCF T_0 values of 3.05 and 3.19 eV for the $1^3A''$ and $1^1A''$ states of the CH_2Cl^+ ion (see Table 6), respectively. As shown in Tables 5 and 6, the geometries of the CH_2Cl fragment in the asymptote products of the $1^2A''$ and $2^2A''$ states are almost identical to the CASSCF geometries of the $1^3A''$ and $1^1A''$ states of the CH_2Cl^+ ion, respectively. We conclude that the $1^2A''$ and $2^2A''$ states of the CH_3Cl^+ ion correlate with the $1^3A''$ and $1^1A''$ states of the CH_2Cl^+ ion, respectively.

As stated above, the $1^2A'$ and $1^2A''$ states, as the two Jahn−Teller splitting states of X^2E, correlate with the different states of the CH_2Cl^+ ion in the H-loss dissociation. Along the CASPT2//CASSCF PECs of the $1^2A'$ and $1^2A''$ states, the energy increases monotonically with the R(C−H_1) value, and there are no barriers (transition states) along the $1^2A'$ and $1^2A''$ PECs. The CASPT2//CASSCF dissociation energies are evaluated (using the relative energy values given in Figure 3) to be 1.95 eV for the CH_3Cl^+ ($1^2A'$) → CH_2Cl^+ (1^1A_1) + H dissociation and 4.97 eV for the CH_3Cl^+ ($1^2A''$) → CH_2Cl^+ ($1^3A''$) + H dissociation. By using the experimental AIP value of 11.29 eV for the X^2E state,[20] the appearance potential for CH_2Cl^+ (1^1A_1) is evaluated to be 13.24 eV, which is quite close to the experimental values of 12.84 eV,[9] 13.0 eV,[8] and 13.05 eV (evaluated by Olney et al.[7] using experimental thermodynamic data). As shown in Figure 3, there exists an energy maximum at an R(C−H_1) value of 1.7 Å along the CASPT2//CASSCF PEC of the $2^2A''$ state, which indicates that there is

TABLE 5: CASPT2//CASSCF Energies (E's) at the Selected R(C−H_1) Values for the H-Loss Dissociation from the $1^2A'$, $1^2A''$, $2^2A'$, and $2^2A''$ States, Together with Charge Values (Q's) on the Departing H_1 Atom and Values of Principal Geometric Parameters in the CASSCF Partially Optimized Geometries[a]

R(C−H_1) (Å)	E (a.u.)	Q(H_1) (e)	R(C−Cl) (Å)	A(H_2CCl) (°)	D(H_2CClH_2') (°)
		$1^2A'$			
1.110	−499.16301	0.326	1.832	106.5	124.6
1.3	−499.15070	0.183	1.781	109.6	131.6
1.7	−499.11130	0.112	1.649	117.9	160.1
2.1	−499.09604	0.042	1.616	119.3	172.9
2.7	−499.09367	0.019	1.607	119.5	178.6
3.0	−499.09313	0.015	1.605	119.5	179.5
4.0	−499.09177	0.004	1.604	119.5	179.9
5.0	−499.09120	0.001	1.604	119.5	180.0
		$1^2A''$			
1.094	−499.16282	0.344	1.835	103.8	115.9
1.3	−499.14203	0.171	1.827	104.5	118.0
1.7	−499.07366	0.097	1.807	106.3	123.2
2.1	−499.02235	0.086	1.785	108.4	129.4
2.7	−498.98928	0.039	1.760	110.6	137.4
3.0	−498.98408	0.023	1.753	111.1	139.4
4.0	−498.98041	0.004	1.747	111.3	139.7
5.0	−498.97984	0.001	1.748	111.4	140.3
		$2^2A'$			
1.6	−499.01679	0.121	1.913	112.4	142.7
1.7	−499.01072	0.092	1.905	112.0	142.9
1.9[b]	−498.99833	0.055	1.888	111.1	143.1
2.1[b]	−498.98668	0.044	1.876	110.4	142.6
2.3[b]	−498.97687	0.045	1.882	109.6	141.6
2.5[c]	−498.96990	0.046	1.887	109.3	141.8
2.7[c]	−498.96456	0.040	1.895	109.2	142.2
3.3[c]	−498.95713	0.016	1.904	109.3	143.9
3.6	−498.95590	0.010	1.904	109.3	143.9
4.0	−498.95515	0.005	1.904	109.4	144.1
5.0	−498.95451	0.001	1.904	109.4	144.1
		$2^2A''$			
1.096	−499.03721	0.373	1.926	114.5	88.2
1.3	−499.01675	0.196	1.921	115.0	89.6
1.6	−498.96545	0.124	1.910	116.1	92.3
1.9	−498.95891	−0.028	1.857	106.8	140.7
2.4	−498.97172	−0.002	1.790	110.6	144.1
3.0	−498.97477	0.008	1.776	111.7	145.9
4.0	−498.97434	0.003	1.772	111.8	146.3
5.0	−498.97390	0.001	1.773	111.8	146.3

[a] For notations, see Figure 1. [b] The H_1CCl angle value was fixed at 111.0°, which is the angle value in the partially optimized geometry at R(C−H) = 1.7 Å. [c] The H_1CCl angle value was fixed at 107.35°, which is the angle value in the partially optimized geometry at R(C−H) = 3.6 Å.

TABLE 6: CASSCF Geometries and CASPT2//CASSCF Relative Energies (T_0's) for the $1^1A'$, $1^3A''$, $1^1A''$, and $1^3A'$ States (the Four Lowest-Lying States) of the CH_2Cl^+ Ion

state	R(C−H) (Å)	R(C−Cl) (Å)	A(HCCl) (°)	D(HCClH′) (°)	T_0 (eV)
$1^1A'$[a]	1.100	1.604	119.5	180.0	0.0
$1^3A''$	1.103	1.747	111.4	140.4	3.05
$1^1A''$	1.100	1.773	111.9	146.5	3.19
$1^3A'$	1.093	1.904	109.4	144.3	3.72

[a] The ground state is 1^1A_1 in C_{2v} symmetry.

TABLE 7: CASPT2//CASSCF Dissociation Energies (D_e's) for Cl Loss and H Loss from the $1^2A'$, $1^2A''$, $2^2A'$, and $2^2A''$ States of the CH_3Cl^+ Ion and CASPT2//CASSCF Appearance Potentials (APs) for the Production of the CH_3^+ and CH_2Cl^+ Ions in Their Ground and Excited States from CH_3Cl

	Cl-loss dissociation			H-loss dissociation		
CH_3Cl^+	product (+Cl)	D_e (eV)	AP (eV)	product (+H)	D_e (eV)	AP (eV)
$1^2A'$	$CH_3^+(1^1A_1')$	2.33	13.62[a] (exptl. 13.33[b], 14.0[c], 13.43[d])	$CH_2Cl^+(1^1A_1)$	1.95	13.24[a] (exptl. 12.84[b], 13.0[c], 13.05[d])
$1^2A''$	$CH_3^+(1^1A_1')$	2.25		$CH_2Cl^+(1^3A'')$	4.97	16.27[a]
$2^2A'$	$CH_3^+(1^1A_1')$	*e*		*f*		
$2^2A''$	$CH_3^+(1^3A'')$	2.48	17.19[a]	$CH_2Cl^+(1^1A'')$	2.36[g]	17.07[h]

[a] Evaluated as the sums of the experimental AIP value of 11.29 eV for the X^2E state (given in ref 20) and the CASPT2//CASSCF relative energies for the asymptote products to the $1^2A'$ reactant (the $1^2A'$ state at the CASSCF equilibrium geometry). [b] From ref 9. [c] From ref 8. [d] Evaluated by Olney et al. (see ref 8) using experimental thermodynamic data. [e] The $2^2A'$ state is repulsive about the C−Cl bond. [f] H-loss dissociation does not occur from $2^2A'$. [g] CASPT2//CASSCF relative energy of the barrier (see text) to the $2^2A''$ reactant. [h] Evaluated as the sum of the experimental AIP value of 11.29 eV for the X^2E state (given in ref 20) and the CASPT2//CASSCF relative energy of the barrier to the $1^2A'$ reactant.

an energy barrier in the CH_3Cl^+ ($2^2A''$) → CH_2Cl^+ ($1^1A''$) + H dissociation reaction. The CASPT2//CASSCF relative energy of the maximum to the $1^2A'$ reactant is 5.78 eV. At the CASPT2//CASSCF level, the maximum is predicted to be 2.36 and 0.63 eV higher in energy than the $2^2A''$ reactant and the asymptote product of the $2^2A''$ state, respectively. It is noted in Table 5 that the H_2CClH_2' dihedral angle value varies drastically in the $R(C-H_1)$ range between 1.6 and 1.9 Å. We note that the dominant configuration in the CASSCF wavefunctions of the $2^2A''$ state is ...$(8a')^2(2a'')^1(9a')^2(10a')^2(3a'')^2$ at the small $R(C-H_1)$ values and it is ...$(8a')^2(2a'')^2(9a')^2(10a')^1$ $(3a'')^1(11a')^1$ at the large $R(C-H_1)$ values. The maximum at $R(C-H_1) = 1.7$ Å along the $2^2A''$ PEC is considered an indication of potential energy surface avoided crossing between two $^2A''$ states, one representing a primary ionized state ($(2a'')^{-1}$) and the other a shake-up ionized state ($(10a')^{-1}(3a'')^{-1}(11a')^1$) (the electron configuration for the ground-state CH_3Cl molecule in C_s symmetry is ...$(8a')^2(2a'')^2(9a')^2(10a')^2(3a'')^2$ $(11a')^0$).

The $2^2A'$ PEC (the $R(C-H_1)$ value ranging from 1.6 to 5.0 Å) shown in Figure 3 is not a true H-loss dissociation PEC. In the CASSCF partial geometry optimization calculations within the $R(C-H_1)$ range from 1.9 to 3.3 Å (the dash−dot part of the $2^2A'$ PEC in Figure 3), the H_1CCl angle was fixed at large values (see the footnotes for Table 5). When we do not fix the H_1CCl angle value in the partial geometry optimization, the H_1 atom moves to the Cl atom and the energy of the system in the $2^2A'$ state goes down (see the dotted line in Figure 3), which indicates that the $2^2A'$ state of the CH_3Cl^+ ion correlates with the CH_2ClH^+ ion (in its ground or excited state). Our calculations support the experimental fact[1,6,7] that the H-loss dissociation does not occur from the $2^2A'$ state of the CH_3Cl^+ ion. We note that the dominant configuration in the CASSCF wavefunction of the $2^2A'$ state is ...$(8a')^2(2A'')^2(9a')^1(10a')^1(3A'')^2(11a')^1$ along the final (solid) part of the $2^2A'$ PEC (within the $R(C-H_1)$ range from 3.6 to 5.0 Å). This means that the final part of the $2^2A'$ PEC is actually a part of the H-loss dissociation PEC of a higher-lying $^2A'$ state, which correlates with the $1^3A'$ state of the CH_2Cl^+ ion. This higher-lying $^2A'$ state represents a shake-up ionized state ($(9a')^{-1}(10a')^{-1}(11a')^1$) at large $R(C-H_1)$ values.

IV. Conclusions

Low-lying electronic states of the CH_3Cl^+ ion have been studied within C_s symmetry by using the CASSCF and CASPT2 methods in conjunction with an ANO basis. On the basis of CASSCF geometry optimization and CASPT2//CASSCF energy calculations, we make the following remarks: The $1^2A'$ state is the ground state, and the $1^2A''$ state is slightly higher in energy (T_0) than $1^2A'$ ($1^2A'$ and $1^2A''$ being the two Jahn−Teller splitting states of X^2E); the $2^2A'$ (A^2A_1) state is a repulsive state about the C−Cl bond, and the CASPT2 T_v' value (3.18 eV) for $2^2A'$ is close to the experimental T_v' value (3.11 eV) for the A $^2A_1$ state; and the CASPT2 T_v' value (4.47 eV) for the $2^2A''$ state is quite close to the experimental T_v' values (4.11 and 4.71 eV) for the B^2E state, while our calculations for the $3^2A'$ state were not successful because of some technical problems ($2^2A''$ and $3^2A'$ being the two Jahn−Teller splitting states of B^2E).

The CASPT2//CASSCF PECs for Cl loss and H loss from the $1^2A'$ (X^2A'), $1^2A''$, $2^2A'$, and $2^2A''$ states were obtained on the basis of the CASSCF partial geometry optimization calculations at the fixed C−Cl and $C-H_1$ distance values, respectively, followed by the CASPT2 energy calculations. The dissociation products (the fragments and their electronic states) were determined by carefully examining the calculation results for the asymptote products (at $R(C-Cl) = R(C-H_1) = 5.0$ Å). In Table 7, we give the CASPT2//CASSCF dissociation energies for the Cl loss and H loss from the different states (for H-loss dissociation from the $2^2A''$ state, we give the CASPT2//CASSCF barrier height value). In Table 7, we give the CASPT2//CASSCF appearance potentials for the ground-state CH_3^+ and CH_2Cl^+ ions, which are in quite good agreement with the experimental values. We also give the CASPT2//CASSCF appearance potentials for the excited-state CH_3^+ and CH_2Cl^+ ions (for the definition, see footnotes a and h for Table 7). on the basis of our CASPT2//CASSCF calculations for the Cl loss and H loss from the four C_s states of the CH_3Cl^+ ion, we will present our conclusions and comments on the general picture (see Introduction) of Eland et al. for the dissociation from the X, A, and B states of the CH_3Cl^+ ion below.

Our CASPT2//CASSCF calculations indicate that the Cl-loss dissociation occurs from the $1^2A'$, $1^2A''$, and $2^2A'$ states of the CH_3Cl^+ ion and the produced CH_3^+ ions are all in the ground state, which supports the observations of direct dissociation from the X and A states of the CH_3Cl^+ ion to CH_3^+ by Eland et al.[1] Our CASPT2//CASSCF calculations indicate that H-loss dissociation does not occur from the $2^2A'$ state, supporting the suggestions of Eland et al.,[1] Lane and Powis,[6] and Olney et al.[8] based on their experiments. Our CASPT2//CASSCF calculations indicate that the H-loss dissociation occurs (with a barrier) from the $2^2A''$ state of the CH_3Cl^+ ion, supporting the observation of direct dissociation from the B state of the CH_3Cl^+ ion to CH_2Cl^+ by Eland et al.[1] and that the produced CH_2Cl^+ ion is in the $1^1A''$ excited state. Our CASPT2//CASSCF calculations indicate that the H-loss dissociation occurs from the $1^2A'$ (X^2A') and $1^2A''$ states of the CH_3Cl^+ ion, and the produced CH_2Cl^+ ion is in the 1^1A_1 (X^1A_1) and $1^3A''$ states, respectively. Apparently, the H-loss dissociation from the two Jahn−Teller splitting states of X^2E should be considered individually.

Acknowledgment. This work was supported by the National Natural Science Foundation Committee of China (nos. 20173056, 20333050).

References and Notes

(1) Eland, J. H. D.; Frey, R.; Kuestler, A.; Schulte, H.; Brehm, B. *Int. J. Mass Spectrom. Ion Phys.* **1976**, *22*, 155.

(2) Werner, A. S.; Tsai, B. P.; Baer, T. *J. Chem. Phys.* **1974**, *60*, 3650.

(3) Baer, T.; Werner, A. S.; Tsai, B. P.; Lin, S. F. *J. Chem. Phys.* **1974**, *61*, 5468.

(4) Orth, R. G.; Dunbar, R. C. *J. Chem. Phys.* **1978**, *68*, 3254.

(5) Carrington, A.; Milverton, D. R. J.; Sarre, P. J. *Mol. Phys.* **1976**, *32*, 297.

(6) Lane, I. C.; Powis, I. *J. Phys. Chem.* **1993**, *97*, 5803.

(7) Won, D. S.; Kim, M. S.; Choe, J. C.; Ha, T.-K. *J. Chem. Phys.* **2001**, *115*, 5454.

(8) Olney, T. N.; Cooper, G.; Chan, W. F.; Burton, G. R.; Brion, C. E.; Tan, K. H. *Chem. Phys.* **1996**, *205*, 421.

(9) Locht, R.; Leyh, B.; Hoxha, A.; Dehareng, D.; Hottmann, K.; Jochims, H. W.; Baumgärtel, H. *Chem. Phys.* **2001**, *272*, 293.

(10) Roos, B. O. In *Ab Initio Methods in Quantum Chemistry, Part 2*; Lawley, K. P., Ed.; Wiley: New York, 1987.

(11) Andersson, K.; Malmqvist, P.-Å.; Roos, B. O.; Sadley, A. J.; Wolinski, K. *J. Phys. Chem.* **1990**, *94*, 5483.

(12) Andersson, K.; Malmqvist, P.-Å.; Roos, B. O. *J. Chem. Phys.* **1992**, *96*, 1218.

(13) Locht, R.; Leyh, B.; Hoxha, A.; Dehareng, D.; Jochims, H. W.; Baumgärtel, H. *Chem. Phys.* **2001**, *272*, 277.

(14) Duflot, D.; Robbe, J.-M.; Flament, J.-P. *J. Chem. Phys.* **1995**, *103*, 10571.

(15) Andersson, K.; Fulscher, M. P.; Lindh, R.; Malmqvist, P.-Å.; Olsen, J.; Sadley, A. J.; Widmark, P.-O. *MOLCAS*, version 5.4; University of Lund: Lund, Sweden, 2002.

(16) Almlöf, J.; Taylor, P. R. *J. Chem. Phys.* **1987**, *86*, 4070.

(17) Widmark, P.-O.; Malmqvist, P.-Å.; Roos, B. O. *Theor. Chim. Acta* **1990**, *77*, 291.

(18) Widmark, P.-O.; Persson, B.-J.; Roos, B. O. *Theor. Chim. Acta* **1990**, *79*, 419.

(19) Jensen, P.; Brodersen, S.; Guelachvili, G. *J. Mol. Spectrosc*. **1981**, *88*, 378.

(20) Karlsson, K.; Jadrny, R.; Mattsson, L.; Chau, F. T.; Siegbahn, K. *Phys. Scr*. **1977**, *16*, 225.